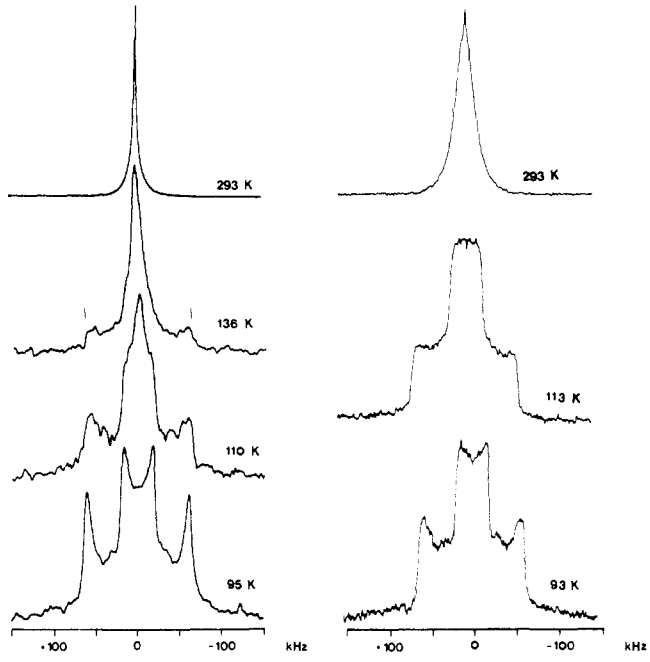


Figure 6. Temperature dependence of the $^2H$ NMR spectra of (–O)-$Si(CH_3)_2(O(C^2H_2)_7C^2H_3)$ with excess hexane at the temperatures indicated together with those of the unsolvated material for comparison (right-hand spectra).

The inability of the solvents, particularly hexane and benzene, to solubilize the surface-immobilized species is also demonstrated by the low-temperature $^2H$ NMR spectra. Figure 6 shows the $^2H$ NMR spectra of the $(-O)Si(CH_3)_2(O(C^2H_2)_7C^2H_3)$ species (D), in the presence of hexane, at a variety of temperatures together with these in the absence of hexane for comparison. At 136 K it is possible to detect a quadrupole pattern for the methylene deuterons with a width of 122 kHz; however, there is still a substantial narrow central component. By 95 K, however, the pattern is fully rigid with a quadrupole splitting of 122 kHz for the methylene deuterons and almost 40 kHz for the $C^2H_3$ group. The presence of substantial motional narrowing at temperatures well below the freezing point of the solvent (178 K) suggests that there is only a limited penetration of the solvent molecules into the surface-immobilized species.

## Conclusions

The current study has demonstrated that $^2H$ NMR is a useful technique for probing the motions of surface-immobilized species. The deuterated alkoxysilanes exhibit motionally narrowed $^2H$ NMR spectra down to temperatures of 150 K, indicating that even in the solid state the alkoxy groups are reorienting quickly ($>10^5$ $s^{-1}$), with the longer chains showing the most motion. Increased motion for longer surface immobilized chains has also been inferred from a solid-state $^{13}C$ NMR relaxation study.[7] The $^2H$ line shapes are not characteristic of any single anisotropic motion but likely represent an isotropic reorientation of the chain with varying torsional motions about the Si–O, C–O, and C–C bonds.

The addition of solvents to the surface-bonded silanes results in further $^2H$ NMR line shape changes. Hexane and benzene induce the formation of a small mobile component whose spectrum is superimposed on a wide line pattern similar to that found in the solid state. However, addition of methanol results in the formation of a larger and essentially isotropic component. Low-temperature studies show that the $^2H$ NMR spectra were still motionally narrowed at temperatures well below the freezing point of the bulk solvent. These observations indicate that hexane and benzene penetrate only to a limited degree into the surface region, while methanol is able to penetrate much more efficiently. Even for the immobilized species with the $C_{14}$ chain, at what are relatively high loading levels, the surface appears to be still quite polar.

**Acknowledgment.** The authors acknowledge the financial assistance of the Natural Sciences and Engineering Research Council of Canada in the form of an Operating Grant (C.A.F.). The NMR spectra were obtained with use of the facilities of the South Western Ontario High Field NMR Centre.

**Registry No.** $ClSi(CH_3)_2(OC^2H_3)$, 100840-07-1; $ClSi(CH_3)_2(OC^2H_2C^2H_3)$, 100857-95-2; $ClSi(CH_3)_2(OC^2H(C^2H_3)_2$, 100840-08-2; $ClSi(CH_3)_2(O(C^2H_2)_7C^2H_3)$, 100840-09-3; $ClSi(CH_3)_2(O(C^2H_2)_{15}C^2H_3)$, 100857-96-3.

# Formation of Electronically Excited Products in Electron-Transfer Reactions: Reaction of Polypyridine Complexes of Cobalt(I) and Ruthenium(III) in Acetonitrile

**David K. Liu, Bruce S. Brunschwig, Carol Creutz, and Norman Sutin***

*Contribution from the Department of Chemistry, Brookhaven National Laboratory, Upton, New York, 11973.* *Received August 23, 1985*

**Abstract:** The yields of the metal-to-ligand charge-transfer excited state of poly(pyridine)ruthenium(II) complexes ($*RuL_3^{2+}$) produced in the reaction of $RuL_3^{3+}$ with poly(pyridine)cobalt(I) complexes in acetonitrile have been measured by use of a combination of continuous flow methods and chemical actinometry. The $*RuL_3^{2+}$ yields are high, ranging from 0.31 ± 0.04 for the most exergonic system ($Ru(bpy)_3^{3+}$ and $Co(4,4'-(CH_3)_2bpy)_3^{+}$) to 0.07 ± 0.02 for the least exergonic system studied ($Ru(4,7-(CH_3)_2phen)_3^{3+}$ and $Co(bpy)_3^{+}$). The results are interpreted in terms of competing electron-transfer channels yielding primarily $*RuL_3^{2+} + CoL_3^{2+}$ and $RuL_3^{2+} + *CoL_3^{2+}$ ($^2T$), with the formation of entirely ground-state products being negligible. A new actinometer consisting of $Os(terpy)_2^{2+}$ and $Co(NH_3)_5Cl^{2+}$, for use at wavelengths up to ~720 nm, is described.

Electron-transfer reactions that are highly exergonic may yield electronically excited rather than ground-state products.[1,2] If the decay of an excited product to its ground state occurs radiatively, then the electron transfer may be accompanied by light emission (chemiluminescence): the intensity of this emission, in turn, provides a convenient measure of the yield of electronically excited products. The relative yields of ground- and excited-state products in highly exergonic reactions is a subject of considerable interest. Not only do the excited-state yields have important implications for electron-transfer theories[2] but also highly exergonic reactions provide a means of generating and characterizing

(1) Rehm, D.; Weller, A. *Isr. J. Chem.* **1970**, *8*, 259.
(2) Siders, P.; Marcus, R. A. *J. Am. Chem. Soc.* **1981**, *103*, 748.

0002-7863/86/1508-1749$01.50/0 

excited states than cannot readily be prepared by direct photoexcitation. Chemiluminescence resulting from electron-transfer reactions of polypyridine–metal complexes has been observed for systems involving product metal-to-ligand charge-transfer excited states ($*RuL_3^{2+}$ and $*OsL_3^{2+}$),[3-6] ligand-field excited states ($*CrL_3^{3+}$ [5,6]), and $\pi-\pi^*$ excited states ($*RhL_2X_2^{+}$ [6]). [L = polypyridine, e.g., 2,2′-bipyridine (bpy) or 1,10-phenanthroline (phen).] Excited $RuL_3^{2+}$ is produced in the reduction of the powerful oxidant $RuL_3^{3+}$,[3-6] in the oxidation of the powerful reductant $RuL_3^{+}$,[7] and in the reaction of $RuL_3^{3+}$ with $RuL_3^{+}$ generated electrochemically.[7-9] Electrogenerated chemiluminescence (ECL) has also been reported for a variety of (polypyridine)osmium complexes.[10]

We have previously studied the quenching of the emission from excited $RuL_3^{2+}$ by $CoL_3^{2+}$ complexes.[11] Oxidative quenching (to produce $RuL_3^{3+}$ and $CoL_3^{+}$) and energy transfer (to produce $RuL_3^{2+}$ and $*CoL_3^{2+}$) were found to be important quenching pathways in these systems. A corollary of the quenching results is that the reaction of $RuL_3^{3+}$ with the powerful reductant $CoL_3^{+}$ should produce $*RuL_3^{2+}$ and that certain of the steps in the chemiluminescence reaction should be identical with those in the quenching reaction. In the present work we report the yield of $*RuL_3^{2+}$ in the reaction of $RuL_3^{3+}$ with $CoL_3^{+}$ complexes in acetonitrile and compare the mechanistic schemes for the quenching and luminescent reactions. The implications of the results for electron-transfer theories are also discussed.

## Experimental Section

**Materials.** The (polypyridine)ruthenium(II) complexes were prepared as in an earlier study.[12] The (polypyridine)ruthenium(III) complexes were isolated as solids[3b] or generated in situ in acetonitrile: in the latter case a few drops of concentrated $HClO_4$ and a spatula tipful of $PbO_2$ were added to a $CH_3CN$ solution (15 mL) of $RuL_3^{2+}$, and the suspension was stirred and filtered through a fine frit. (Polypyridine)cobalt(II) complexes were prepared as previously described,[13] and stock solutions of the cobalt(I) complexes were prepared by electrochemical reduction on Pt gauze of 0.03 M solutions of the corresponding cobalt(II) complexes (prepared either from the solids or by dissolving $Co(ClO_4)_2 \cdot 6H_2O$ and L in a ratio of 1 to 3.3) in acetonitrile at ~−1.1 V vs. SCE: 0.1 M tetraethylammonium perchlorate (TEAP) was usually also present and the solutions were magnetically stirred under a blanket of argon during the electrolysis, which normally lasted about 2 h. The yield of $CoL_3^{+}$ was typically 70%. $[Os(terpy)_2]Cl_2$ was prepared by a method similar to that reported in the literature,[14] and $[Co(NH_3)_5Cl]Cl_2$ was from an earlier study.[15a] All the polypyridine ligands were from Aldrich or G. F. Smith and were used as received. $RuCl_3 \cdot 1\text{-}3H_2O$ (Alfa) and $Co(ClO_4)_2 \cdot 6H_2O$ (G. F. Smith) were used without further purification. Tetraethylammonium perchlorate was obtained from Kodak and was recrystallized from acetonitrile before use. Acetonitrile was HPLC grade from Fisher and was dried over molecular sieves (Aldrich, 3A, 8–12 mesh) prior to use.

**Molar Absorptivities of the Co(I) Complexes.** The molar absorptivities of the Co(I) complexes were determined by measuring the absorbance changes upon addition of aliquots of concentrated solutions of the corresponding Co(III) complexes to the Co(I) solutions ($2 \times 10^{-4}$ M) in acetonitrile. Plots of absorbance vs. added [Co(III)] yielded straight lines with slopes equal to $(2\epsilon_{Co(II)} - \epsilon_{Co(I)})l$ and intercepts equal to $[Co(I)]_0\epsilon_{Co(I)}l$, where $[Co(I)]_0$ is the initial Co(I) concentration and $l$ is the path length of the cell (1.0 cm).

**Electrochemical Measurements.** Controlled-potential electrolysis was carried out with a PAR Model 173 potentiostat, and cyclic voltammetry was performed with either a Model 173 potentiostat and a Model 175 universal programmer or a BAS-100 electrochemical analyzer, using Pt working and auxiliary electrodes in a conventional three-electrode arrangement with a saturated calomel reference electrode.

**Quenching Measurements.** Emission spectra were recorded on a Perkin-Elmer MPF4 spectrofluorimeter. Quenching rate constants were obtained either from Stern–Volmer plots of the emission intensity data as a function of the quencher concentration or from lifetime studies using the frequency-doubled neodymium laser described previously.[12]

**Chemiluminescence Spectra.** Spectra of the emission from the reaction of $CoL_3^{+}$ with $RuL_3^{3+}$ were recorded on a Princeton Instruments spectrometric multichannel analyzer (SMA) equipped with a 512-element Reticon-type photodiode array. The SMA was mounted on a 0.32-m monochromator and light from 560 to 820 nm could be detected. A four-jet mixing chamber and flow tube were mounted directly in front of the entrance slit of the monochromator. For purposes of comparison, the emission spectrum of $Ru(bpy)_3^{2+}$ in acetonitrile, excited with 450-nm light from a xenon lamp, was also recorded.

**Emission Actinometry.** The number of photons produced in the reaction was determined by use of an $Os(terpy)_2^{2+}/Co(NH_3)_5Cl^{2+}$ actinometer. This actinometer is similar to the $Ru(bpy)_3^{2+}/Co(NH_3)_5Cl^{2+}$ actinometer previously described[15] except that the $Ru(bpy)_3^{2+}$ was replaced by $Os(terpy)_2^{2+}$ ($\epsilon_{620} \sim 3.5 \times 10^3$ $M^{-1}$ $cm^{-1}$) because osmium(II)–polypyridine complexes absorb strongly in the region of the $*RuL_3^{2+}$ emission and $*Os(terpy)_2^{2+}$, a relatively long-lived (0.14 μs) MLCT excited state, is efficiently and irreversibly quenched by $Co(NH_3)_5Cl^{2+}$.[15b] The actinometer was calibrated as follows: Deaerated 0.5 M $H_2SO_4$ solutions containing $1.9 \times 10^{-4}$ M $Os(terpy)_2^{2+}$ and $1 \times 10^{-2}$ M $Co(NH_3)_5Cl^{2+}$ were photolyzed in 2-cm cylindrical cells using 480- or 620-nm light (±10-nm band-pass filters) from a 450-W xenon lamp, and the loss of osmium(II) absorbance at 656 nm ($\epsilon_{Os(II)} - \epsilon_{Os(III)} = 2.50 \times 10^3$ $M^{-1}$ $cm^{-1}$) was monitored. The light intensity was determined with a calibrated Eppley thermopile (Model 21433). The net reaction occurring in the actinometer is

$$Os(terpy)_2^{2+} + Co(NH_3)_5Cl^{2+} + h\nu \xrightarrow{H^+} Os(terpy)_2^{3+} + Co^{2+} + 5NH_4^{+} + Cl^{-}$$

and the effective quantum yield $\Phi_a$ for the formation of $Os(terpy)_2^{3+}$ (corrected for the fraction of incident light not absorbed by $Os(terpy)_2^{2+}$ at the appropriate wavelength) was determined to be 0.54 ± 0.09 under the conditions used. The value of $\Phi_a$ is equal to the product of the number of $*Os(terpy)_2^{2+}$ produced per photon absorbed, the fraction of $*Os(terpy)_2^{2+}$ quenched by $Co(NH_3)_5Cl^{2+}$ ($K_{SV}[Co(III)]/[1 + K_{SV}[Co(III)]]$), and the yield of $Os(terpy)_2^{3+}$ in the quenching reaction. The Stern–Volmer constant $K_{SV}$ for the quenching of the $*Os(terpy)_2^{2+}$ emission by $Co(NH_3)_5Cl^{2+}$ was determined to be 125 ± 12 $M^{-1}$ in 0.50 M $H_2SO_4$ so that the fraction of $Os(terpy)_2^{2+}$ excited states quenched by $Co(NH_3)_5Cl^{2+}$ at the Co(III) concentration used is 0.56 ± 0.02. Since the value of $\Phi_a$ is equal to this value within the experimental error of the measurements, the yield of $Os(terpy)_2^{3+}$ in the quenching reaction and the yield of $*Os(terpy)_2^{2+}$ are both close to unity. In subsequent applications, the value of $\Phi_a$ will therefore be assumed equal to the fraction of $Os(terpy)_2^{2+}$ excited states quenched by $Co(NH_3)_5Cl^{2+}$.

**Chemiluminescence Measurements.** The apparatus for the chemiluminescence studies employed a flow system similar to those previously described.[16] The pistons of the two reactant syringes (20 mL) were driven by a Harvard 944 infusion-withdrawal pump (combined flow rate of 0.7 mL per s). The syringes were attached to three-way stopcocks that could be used either to admit the reactant solutions or to deliver them into the reaction cell or into a spectrophotometer cell for the determination of the reactant concentrations. The reaction cell consisted of a two-jet mixing chamber followed by a 1-mm-i.d., 5-cm-long, U-shaped flow tube mounted in a male joint. Chemiluminescence was observed in

(3) (a) Lytle, F. E.; Hercules, D. M. *Photochem. Photobiol.* **1971**, *13*, 123. (b) Ghosh, P.; Brunschwig, B. S.; Chou, M.; Creutz, C.; Sutin, N. *J. Am. Chem. Soc.* **1984**, *106*, 4772.
(4) Martin, J. E.; Hart, E. J.; Adamson, A. W.; Gafney, H.; Halpern, J. *J. Am. Chem. Soc.* **1972**, *94*, 9238. Jonah, C. D.; Matheson, M. S.; Meisel, D. *J. Am. Chem. Soc.* **1978**, *100*, 1449.
(5) Balzani, V.; Bolletta, F. *J. Photochem.* **1981**, *17*, 479. Balzani, V.; Bolletta, F.; Ciano, M.; Maestri, M. *J. Chem. Educ.* **1983**, *60*, 447. Balzani, V.; Bolletta, F. *Comments Inorg. Chem.* **1983**, *2*, 211.
(6) Vogler, A.; El-Sayed, L.; Jones, R. G.; Namnath, J.; Adamson, A. W. *Inorg. Chim. Acta* **1981**, *53*, L35. Gafney, H. D.; Adamson, A. W. *J. Chem. Educ.* **1975**, *52*, 480.
(7) Tokel-Takvoryan, N. E.; Hemingway, R. E.; Bard, A. J. *J. Am. Chem. Soc.* **1973**, *95*, 6582.
(8) (a) Wallace, W. L.; Bard, A. J. *J. Phys. Chem.* **1979**, *83*, 1350. (b) Rubinstein, I.; Bard, A. J. *J. Am. Chem. Soc.* **1981**, *103*, 512. (c) Itoh, K.; Honda, K. *Chem. Lett.* **1979**, 99.
(9) Glass, R. S.; Faulkner, L. R. *J. Phys. Chem.* **1981**, *85*, 1160.
(10) Abruña, H. D. *J. Electrochem. Soc.* **1985**, *132*, 842. Abruña, H. D. *J. Electroanal. Chem.* **1984**, *175*, 321.
(11) Krishnan, C. V.; Brunschwig, B. S.; Creutz, C.; Sutin, N. *J. Am. Chem. Soc.* **1985**, *107*, 2005.
(12) Lin, C.-T.; Böttcher, W.; Chou, M.; Creutz, C.; Sutin, N. *J. Am. Chem. Soc.* **1976**, *98*, 6536.
(13) Burstall, F. H.; Nyholm, R. S. *J. Chem. Soc.* **1952**, 3570.
(14) Creutz, C.; Chou, M.; Netzel, T. L.; Okumura, M.; Sutin, N. *J. Am. Chem. Soc.* **1980**, *102*, 1309.
(15) (a) Chan, S.-F.; Chou, M.; Creutz, C.; Matsubara, T.; Sutin, N. *J. Am. Chem. Soc.* **1981**, *103*, 369. (b) Navon, G.; Sutin, N. *Inorg. Chem.* **1974**, *13*, 2159.
(16) (a) Dulz, G.; Sutin, N. *Inorg. Chem.* **1963**, *2*, 917. (b) Sutin, N.; Gordon, B. M. *J. Am. Chem. Soc.* **1961**, *83*, 70.

**Table I.** Reduction Potentials (V) for Polypyridine Complexes Used in this Study[a]

| | ground state | | excited state | |
|---|---|---|---|---|
| | $E°_{3,2}$ | $E°_{2,1}$ | $*E°_{3,2}$ | $*E°_{2,1}$ |
| $Ru(bpy)_3^{2+}$ | +1.29 | −1.28 | −0.81 | +0.84 |
| $Ru(4,7\text{-}(CH_3)_2phen)_3^{2+}$ | +1.12 | −1.47 | −0.98 | +0.67 |
| $Os(terpy)_2^{2+}$ | +0.91[b] | −1.28[d] | −0.86[b,c] | +0.49[c,d] |
| $Co(bpy)_3^{2+}$ | +0.30 | −0.98 | | |
| $Co(4,4'\text{-}(CH_3)_2bpy)_3^{2+}$ | +0.18 | −1.10 | | |
| $Co(terpy)_2^{2+}$ | +0.26[d] | −0.87[d] | | |

[a] Values for $RuL_3^{2+}$ and $CoL_3^{2+}$ from ref 22, 12, and 11, in acetonitrile vs. SCE unless otherwise noted. [b] Values appropriate to aqueous media, vs. NHE. This work, in 0.5 M $H_2SO_4$. [c] Calculated from the ground-state potential by using an excited-state energy of 1.77 eV (see Demas, J. N.; Crosby, G. A. *J. Am. Chem. Soc.* **1971**, *93*, 2841). [d] Determined in this work in acetonitrile containing 0.1 M tetraethylammonium perchlorate.

only the first few millimeters of the flow tube. The mixing chamber and flow tube were positioned in a cylindrical vessel (female 34/45 joint) containing about 40 mL of actinometer solution composed of $Os(terpy)_2^{2+}$ ($5.5 \times 10^{-4}$ M) and $Co(NH_3)_5Cl^{2+}$ ($1.5 \times 10^{-2}$ M) in 0.5 M $H_2SO_4$. The cylindrical vessel, in turn, stood in a 100-mL beaker with silvered outside walls. The minimum path length of actinometer solution surrounding the reaction cell was 1.5 cm, corresponding to an Os(II) absorbance of more than 2.0 at 620 nm.

All chemiluminescence experiments were performed in a darkened room. In a typical experiment, 200 mL of solvent in each reaction vessel was purged with Ar for 1 h prior to the introduction of aliquots of stock solutions of the $CoL_3^+$ and $RuL_3^{3+}$ complexes. The resultant concentrations of the reactants were generally $<2 \times 10^{-3}$ M, with $CoL_3^+$ being the limiting reagent. The reactant solutions were drawn into the syringes through the three-way stopcocks, the reaction cell was rinsed several times by flowing the reactant solutions through the cell, and the rinsings were discarded. Small portions of the reactant solutions were then separately drained into two spectrophotometer cells for the determination of the reactant concentrations. The actinometer solution was then introduced into the vessel surrounding the reaction cell, and the withdrawal–infusion cycle was performed until the reactant solutions were exhausted, at which time the volume of the reaction mixture was determined (generally about 300 mL).

The number of photons produced in the reaction of $RuL_3^{3+}$ with $CoL_3^+$ was determined by measuring the amount of $Os(terpy)_2^{3+}$ produced in the actinometer solution as follows: after the completion of the flow sequence the actinometer solution was passed sequentially through four Sep-Pak $C_{18}$ cartridges (Water Associates, Milford, MA) that had been washed with 5 mL of $CH_3CN$ followed by 10 mL of $H_2O$. The $Os(terpy)_2^{2+}$ was retained on the Sep-Pak cartridges as a dark-brown band. The pink eluate containing $Os(terpy)_2^{3+}$, $Co(NH_3)_5Cl^{2+}$, and $Co^{2+}$ was treated with excess ammonium thiocyanate, which reduced the $Os(terpy)_2^{3+}$. The $Os(terpy)_2^{2+}$ thus formed was collected on a pretreated Sep-Pak cartridge, which was then washed with 5 mL of $H_2O$ to remove the Co species, and finally eluted with $CH_3CN$. The $CH_3CN$ eluate was diluted to 5.00 mL, and the amount of $Os(terpy)_2^{2+}$ was determined from the volume and absorbance of the eluate ($\epsilon$ $1.38 \times 10^4$ $M^{-1}$ $cm^{-1}$ at 474 nm). In control experiments, 97 ± 3% of the initial $Os(terpy)_2^{3+}$ was recovered from a simulated actinometer mixture.

## Results

The reduction potentials of the (polypyridine)ruthenium and -cobalt complexes studied in this work are summarized in Table I. It is evident from the reduction potentials that the Ru(III) and Co(I) complexes are very strong oxidants and reductants, respectively,[17] and the trends in potentials have been discussed previously.[11,22] The absorption spectra, excited-state emission spectra, and lifetimes of the excited states are presented in Table II and are in good agreement with those previously reported.[12,23,24] While $CoL_3^{2+}$ does not absorb appreciably in the visible region, $Co(terpy)_2^{2+}$ exhibited several rather intense absorption maxima ($\epsilon \sim 10^3$ $M^{-1}$ $cm^{-1}$) in the same region. None of the Co(II) complexes exhibited detectable emission at room temperature or at 77 K.

**Table II.** Absorption and Emission Maxima for Polypyridine Complexes Used in This Study[a]

| | absorption $\lambda_{max}$, nm ($10^{-4}$ $\epsilon$, $M^{-1}$ $cm^{-1}$) | emission[b] $\lambda_{max}$, nm ($\tau$, $\mu$s) |
|---|---|---|
| $Ru(bpy)_3^{2+}$ | 350 sh, 428 sh, 450 (1.51) | 607 (0.85) |
| $Ru(bpy)_3^{3+}$ | 415 (0.24), 665 (0.075) | |
| $Ru(4,7\text{-}(CH_3)_2phen)_3^{2+}$ | 428 (1.44), 445 (1.45) | 597 (1.1) |
| $Ru(4,7\text{-}(CH_3)_2phen)_3^{3+}$ | 338 (1.37), 356 (1.49), 413 sh, 680 (0.18) | |
| $Os(terpy)_2^{2+}$ | 310 (6.73), 474 (1.38), 656 (0.37) | 713 (0.14)[c] |
| $Os(terpy)_2^{3+}$ | 470 sh, 506 (0.081), 652 (0.12) | |
| $Co(bpy)_3^+$ | 376 (0.43), 605 (0.58) | |
| $Co(4,4'\text{-}(CH_3)_2bpy)_3^+$ | 396 (0.49), 612 (0.55) | |
| $Co(terpy)_2^{2+}$ | 415 (0.15), 443 (0.15), 503 (0.12), 550 (0.046) | |
| $Co(terpy)_2^+$ | 427 (0.65), 555 (0.49) | |

[a] All measurements were in acetonitrile unless otherwise noted. [b] Uncorrected emission maximum measured on the MPF4. Emission was detected only for the Ru(II) and Os(II) complexes. [c] Lifetime in 0.5 M $H_2SO_4$.

**Table III.** Rate Constants for the Quenching of $RuL_3^{2+}$ and $OsL_3^{2+}$ Emission in Acetonitrile Containing 0.10 M Tetraethylammonium Perchlorate at 25 °C[a]

| $*ML_3^{2+}$ | quencher | $10^{-9}k_q$, $M^{-1}$ $s^{-1}$ |
|---|---|---|
| $Ru(bpy)_3^{2+}$ | $Co(bpy)_3^+$ | 6.6 |
| $Ru(bpy)_3^{2+}$ | $Co(4,4'\text{-}(CH_3)_2bpy)_3^+$ | 2.7 |
| $Ru(bpy)_3^{2+}$ | $Co(terpy)_2^+$ | 2.0 |
| $Ru(4,7\text{-}(CH_3)_2phen)_3^{2+}$ | $Co(bpy)_3^+$ | 3.8 |
| $Ru(bpy)_3^{2+}$ | $Co(bpy)_3^{2+}$ | 0.11 (0.08[b])[c] |
| $Ru(bpy)_3^{2+}$ | $Co(4,4'\text{-}(CH_3)_2bpy)_3^{2+}$ | 0.16[c] |
| $Ru(bpy)_3^{2+}$ | $Co(terpy)_2^{2+}$ | 3.3[c] |
| $Ru(4,7\text{-}(CH_3)_2phen)_3^{2+}$ | $Co(bpy)_3^{2+}$ | 0.19[c] |
| $Ru(bpy)_3^{2+}$ | $Ru(bpy)_3^{3+}$ | 3.2 |
| $Ru(4,7\text{-}(CH_3)_2phen)_3^{2+}$ | $Ru(4,7\text{-}(CH_3)_2phen)_3^{3+}$ | 2.5 |
| $Os(terpy)_2^{2+}$ | $Co(NH_3)_5Cl^{2+}$ | 0.87[d] |

[a] Rate constants from lifetime measurements unless otherwise indicated. [b] In 0.01 M tetraethylammonium perchlorate. [c] From steady-state emission intensity measurements. [d] Rate constant in 0.5 M $H_2SO_4$.

Rate constants for the quenching of $*RuL_3^{2+}$ by $CoL_3^+$, $CoL_3^{2+}$, $Co(terpy)_2^{2+}$, and $RuL_3^{3+}$ are presented in Table III. The rate constants for the quenching of $*RuL_3^{2+}$ by the Co(II) complexes were determined from Stern–Volmer plots of the emission intensity as a function of Co(II) concentration after correcting the intensities for the absorbance of the donor and quencher. In the cases where $CoL_3^+$ or $RuL_3^{3+}$ was the quencher, lifetimes rather than emission intensities were measured because of the high absorption of the $CoL_3^+$ and the instability of $RuL_3^{3+}$ (with respect to the formation of $RuL_3^{2+}$).[25a]

**Chemiluminescence Yields.** Orange-red chemiluminescence was observed with all the Ru(III) and Co(I) complexes used in this study.[25b] In Figure 1 the spectrum of the emission resulting from the reaction of $Ru(bpy)_3^{3+}$ with $Co(bpy)_3^+$ in acetonitrile is

(17) In fact, it has been shown that $RuL_3^{3+}$ is capable of oxidizing water to $O_2$ in the presence of added catalyst such as $Co^{2+}_{(aq)}$,[3b,18,19] and that $CoL_3^+$ can reduce water to $H_2$[11] and $CO_2$ to CO,[20,21] depending upon experimental conditions.

(18) Shafirovich, V. Ya.; Khannanov, N. K.; Strelets, V. V. *Nouv. J. Chim.* **1980**, *4*, 81.
(19) Brunschwig, B. S.; Chou, M. H.; Creutz, C.; Ghosh, P.; Sutin, N. *J. Am. Chem. Soc.* **1983**, *105*, 4832.
(20) Keene, F. R.; Creutz, C.; Sutin, N. *Coord. Chem. Rev.* **1985**, *64*, 247.
(21) Lehn, J.-M.; Ziessel, R. *Proc. Natl. Acad. Sci. U.S.A.* **1982**, *79*, 701.
(22) Sutin, N.; Creutz, C. *Adv. Chem. Ser.* **1978**, *No. 168*, 1.
(23) Young, R. C.; Meyer, T. J.; Whitten, D. G. *J. Am. Chem. Soc.* **1976**, *98*, 286.
(24) Hauenstein, B. L., Jr.; Dressick, W. J.; Buell, S. L.; Demas, J. N.; DeGraff, B. A. *J. Am. Chem. Soc.* **1983**, *105*, 4251.
(25) (a) Liu, D. K.; Sutin, N. unpublished results. See also ref 3b. (b) The chemiluminescence from the reaction of $Ru(bpy)_3^{3+}$ with $Co(bpy)_3^+$ was first observed in our laboratories by F. R. Keene and J. R. Winkler.

Table IV. Chemiluminescene Yields for the Reaction of $RuL_3^{3+}$ with $CoL_3^{+}$ in Acetonitrile Containing 0.1 M Tetraethylammonium Perchlorate at 25 °C

| reactants | $-\Delta G°$(*Ru),[a] eV | [Ru(III)],[b] mM | [(Co(I)],[b] mM | [Co(II)],[b] mM | $10^2Y$(*Os)[c] | $10^2Y_{h\nu}$[d] | $Y$(*Ru)[e] |
|---|---|---|---|---|---|---|---|
| $Ru(bpy)_3^{3+}$ + $Co(4,4'\text{-}(CH_3)_2bpy)_3^{+}$ | 0.29 | 0.80 | 0.16 | 0.08 | 0.74 | 0.79 | 0.33 |
| | | 0.80 | 0.17 | 0.09 | 0.60 | 0.67 | 0.28 |
| | | 0.90 | 0.09 | 0.055 | 0.65 | 0.71 | 0.33 |
| $Ru(bpy)_3^{3+}$ + $Co(bpy)_3^{+}$ | 0.17 | 0.45 | 0.10 | 0.04 | 0.66 | 0.70 | 0.22 |
| | | 0.55 | 0.075 | 0.02 | 0.49 | 0.52 | 0.18 |
| | | 0.55 | 0.13 | 0.03 | 0.68 | 0.73 | 0.26 |
| $Ru(bpy)_3^{3+}$ + $Co(terpy)_2^{+}$ | 0.06 | 0.60 | 0.16 | 0.07 | 0.33 | 0.35 | 0.14 |
| | | 0.65 | 0.25 | 0.10 | 0.23 | 0.27 | 0.12 |
| | | 0.70 | 0.20 | 0.09 | 0.27 | 0.30 | 0.14 |
| $Ru(4,7\text{-}(CH_3)_2phen)_3^{3+}$ + $Co(bpy)_3^{+}$ | 0 | 0.55 | 0.12 | 0.03 | 0.17 | 0.19 | 0.07 |
| | | 0.55 | 0.20 | 0.05 | 0.10 | 0.12 | 0.05 |
| | | 0.60 | 0.08 | 0.02 | 0.20 | 0.23 | 0.10 |

[a] Standard free energy change for the formation of $*Ru(bpy)_3^{2+}$ and $Co(bpy)_3^{2+}$. [b] Initial concentrations in the reaction mixture. [c] Number of moles of $*Os(terpy)_2^{2+}$ produced in the actinometer per mole of Co(I). In computing this ratio from the $Os(terpy)_2^{3+}$ yield a correction (0.65) has been made for the fraction of $Os(terpy)_2^{2+}$ excited states not quenched by $Co(NH_3)_5Cl^{2+}$. [d] Number of moles of photons produced per mole of Co(I). Calculated from $Y$(*Os) by introducing a correction for the absorption of $*RuL_3^{2+}$ emission by the solution in the flow tube. [e] Number of moles of $*RuL_3^{2+}$ produced per mole of Co(I). Calculated from $Y_{h\nu}$ by correcting for the emission yield of $*RuL_3^{2+}$ and for quenching of the $*RuL_3^{2+}$ emission. The latter correction is $1 + \sum K_{SV}[\bar{Q}]$, where $[\bar{Q}]$ is the average concentration of the quencher during the run.

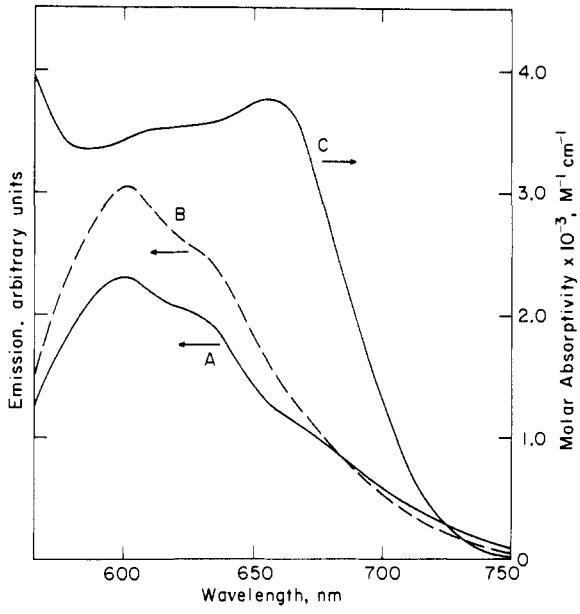


Figure 1. (A) Spectrum of the emission arising from the reaction of $5 \times 10^{-4}$ M $Ru(bpy)_3^{3+}$ with $5 \times 10^{-4}$ M $Co(bpy)_3^{+}$ in acetonitrile containing 0.1 M tetraethylammonium perchlorate. (B) Emission spectrum of $5 \times 10^{-5}$ M $Ru(bpy)_3^{2+}$ in acetonitrile produced by excitation with 450-nm light. (C) Absorption spectrum of $Os(terpy)_2^{2+}$ in water.

compared with that produced upon photoexcitation of $Ru(bpy)_3^{2+}$. The absorption spectrum of $Os(terpy)_2^{2+}$ used in the actinometer is also included. The emission spectra are very similar (the apparent shoulder at ~670 nm in the chemiluminescence spectrum is due to the $Co(bpy)_3^{+}$ absorbance at lower wavelengths), establishing that the emission in the chemiluminescent reaction is from the MLCT state of $Ru(bpy)_3^{2+}$. This assignment is consistent with earlier studies[3-6] and with the fact that the cobalt(II) products do not emit detectably at room temperature. A summary of the experimental results that shows the reaction partners, the free energy change of the reaction leading to the formation of $*RuL_3^{2+}$, and the photon and excited-state yields is given in Table IV. The latter yields are based upon the number of moles of $CoL_3^{+}$ (the limiting reagent) taken. The photon yield was calculated by dividing the number of moles of $Os(terpy)_2^{3+}$ produced in the actinometer by the efficiency of the actinometer (65% at the $Co(NH_3)_5Cl^{2+}$ concentration used) and correcting for the absorption of the chemiluminescence radiation in the reaction mixture (6–12%, depending on the system). The excited-state yield was calculated by dividing the photon yield by the (unquenched) emission yield of the excited state (0.075 for $Ru(bpy)_3^{2+}$ [8a] and 0.065 for $Ru(4,7\text{-}(CH_3)_2phen)_3^{2+}$ [26a]) and multiplying it by $(1 + \sum K_{SV}[\bar{Q}])$ where $[\bar{Q}]$ is the average concentration of a particular quencher ($RuL_3^{3+}$, $CoL_3^{+}$, or $CoL_3^{2+}$) in the reaction mixture. The latter factor, which corrects for the quenching of the $RuL_3^{2+}$ emission in the reaction mixture, was generally of the order of 2–3 and was largely determined by the $RuL_3^{3+}$ concentration. The $RuL_3^{3+}$ was present in sufficient excess that its concentration remained essentially constant during a given run.

## Discussion

The yield of excited-state $RuL_3^{2+}$ increases with the exergonicity of the reaction: the yield is fairly high (31 ± 4%) for reaction of $Ru(bpy)_3^{3+}$ with $Co(4,4'\text{-}(CH_3)_2bpy)_3^{+}$, which is the most exergonic of the reactions studied ($\Delta G°(Ru^*) = -0.29$ eV), and quite low (~7 ± 2%) for the least exergonic reaction. It is noteworthy that although the $Ru(bpy)_3^{3+}$–$Co(terpy)_2^{+}$ system is complicated by the presence of a low-spin/high-spin equilibrium for $Co(terpy)_2^{2+}$,[26b] the chemiluminescence yield correlates with the yields for the bpy and phen cobalt(I) complexes. The high excited-state yields in these systems presumably derive from the fact that the reaction to form ground-state $RuL_3^{2+}$ (eq 1) is so

$$RuL_3^{3+} + CoL_3^{+} \rightarrow RuL_3^{2+} + CoL_3^{2+} \quad (1)$$

$$RuL_3^{3+} + CoL_3^{+} \rightarrow *RuL_3^{2+} + CoL_3^{2+} \quad (2)$$

exergonic that it lies in the inverted region ($-\Delta G° > \lambda$, where $\lambda$ is the reorganization parameter) and, as a consequence, proceeds relatively slowly. On the other hand, because of its much smaller exergonicity, the reaction to form excited-state $*RuL_3^{2+}$ (eq 2) lies in the normal free energy region ($-\Delta G° < \lambda$) and can therefore proceed rapidly. Provided that all other factors are equal, the ratio of the rate constants, calculated from the Marcus expressions,[27] for reactions 1 and 2 is given by

$$\log\left(\frac{k_2}{k_1}\right) = \frac{(\Delta G_1° - \Delta G_2°)}{4.6RT}\left[1 + \frac{(\Delta G_1° + \Delta G_2°)}{2\lambda}\right] \quad (3)$$

where $\lambda$ is assumed to be the same for the two reactions. For the reaction of $Ru(bpy)_3^{3+}$ with $Co(4,4'\text{-}(CH_3)_2bpy)_3^{+}$, which has the highest excited-state yield, $\Delta G_1° = -2.4$ eV and $\Delta G_2° = -0.3$ eV so that, for $\lambda = 0.8$ eV,[28a] $k_2/k_1 \sim 10^{12}$. In view of the large

(26) (a) The emission quantum yield of $Ru(4,7\text{-}(CH_3)_2phen)_3^{2+}$ was determined to be 0.065 in acetonitrile based on the relative emission intensity of $Ru(4,7\text{-}(CH_3)_2phen)_3^{2+}$ and $Ru(bpy)_3^{2+}$ solutions that had been prepared to give the same absorbance at 450 nm; an emission quantum yield of 0.075 for $Ru(bpy)_3^{2+}$ in acetonitrile at 25 °C was used.[8a] The lower emission yield of $Ru(4,7\text{-}(CH_3)_2phen)_3^{2+}$ is surprising in view of the longer lifetime of its excited state. (b) Kremer, S.; Henke, W.; Reinen, D. *Inorg. Chem.* **1982**, *21*, 3013.

(27) Marcus, R. A. *Annu. Rev. Phys. Chem.* **1964**, *15*, 155.

**Scheme I**

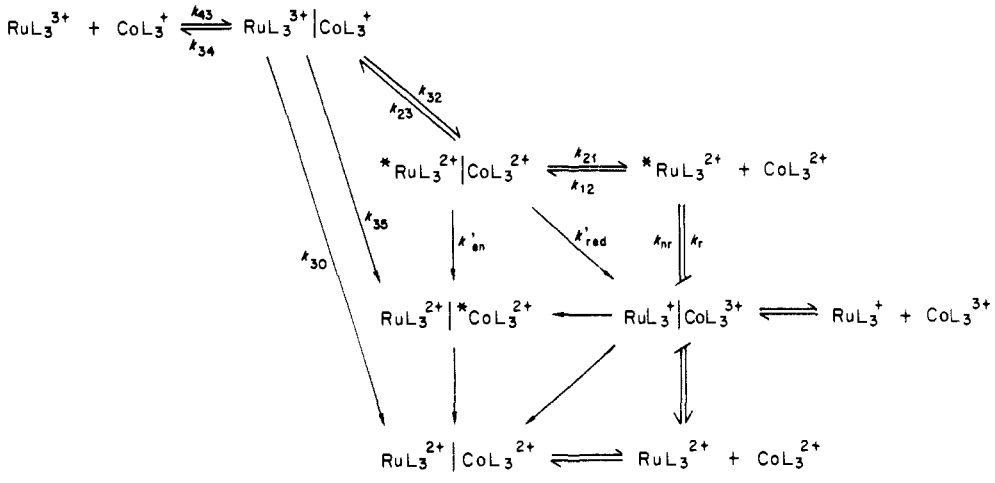

difference in the rates calculated for formation of ground- and excited-state $RuL_3^{2+}$, the question posed by these studies is not why the excited-state yields are as high as they are but rather why the yields are significantly below 100%.[28c]

One possible explanation for the less than quantitative formation of $*RuL_3^{2+}$ is the breakdown of the Marcus expressions in the inverted region, resulting in an underestimate of the rate of the reaction forming ground-state products. Various reasons for such a breakdown have been considered,[3,29,30] but none is entirely satisfactory. For example, nuclear tunneling effects are not included in the classical expressions: however, although such corrections can be large (particularly for reactions in the inverted region), substantial rate decreases are still predicted for systems of the type studied here. Nor does a change in mechanism (to, e.g., hydrogen atom transfer) seem reasonable for the present systems. However a very real possibility for the systems under discussion is the existence of additional reaction channels involving the formation of excited-state $CoL_3^{2+}$ (eq 4). Reasonable can-

$$RuL_3^{3+} + CoL_3^{+} \rightarrow RuL_3^{2+} + *CoL_3^{2+} \qquad (4)$$

didates for $*CoL_3^{2+}$ when L = bpy or 4,4'-$(CH_3)_2$bpy are the $^2T$, $^4T_2$, and/or $^2E$ states of $CoL_3^{2+}$, *all* of which are energetically accessible in the Ru(III)/Co(I) reaction.

The properties of $CoL_3^{2+}$ excited states are summarized in Table V. The transition energies and the assignment of the $^2T$ and $^4T_2$ excited states are taken from the literature,[31] while the (vertical) energy of the $^2E$ state was estimated by using the *Dq* and *B* parameters derived from the $^2T$ and $^4T_2$ states. The formation of the $^2T$ state from the ground state does not involve a change in the population of the $\sigma^*$d orbitals: as a consequence the excited state is unlikely to be distorted relative to the ground state and we have assumed that the energy of the thermally equilibrated $^2T$ state is equal to the transition energy. Similarly, the rate constant and electronic transmission coefficient for electron exchange of the $^2T$ state with $Co(bpy)_3^+$ is assumed equal to the values for the $Co(bpy)_3^{2+}/Co(bpy)_3^+$ ground-state exchange. On the other hand, there is a change in the population of the $\sigma^*$d orbitals in forming the $^4T_2$ state, and as a consequence the cobalt–nitrogen distances are likely to be about 0.10–0.12 Å longer in the excited state than in the $Co(bpy)_3^{2+}$ ground state.[32] On this basis the thermally equilibrated $^4T_2$ state is estimated to lie ~0.3 eV below the Franck–Condon state[33] and therefore ~1.1 eV above the ground state. The exchange rate for this couple can be estimated as follows. The exchange rate of the ground-state $Co(bpy)_3^+/Co(bpy)_3^{2+}$ couple is $\sim 1 \times 10^9$ $M^{-1}$ $s^{-1}$ at 0.1 M ionic strength. The cobalt–nitrogen distances are ~0.02 Å longer in $Co(bpy)_3^{2+}$ than in $Co(bpy)_3^+$,[28b] while, as noted above, the cobalt–nitrogen distances are likely to be 0.10–0.12 Å longer in the excited state than in $Co(bpy)_3^{2+}$. The difference in the cobalt–nitrogen distances will contribute an additional barrier of ~0.2 eV to the excited-state electron-transfer reaction compared with the ground-state exchange. In addition, because the electron exchange cannot be effected simply by the transfer of a single electron, the excited-state exchange is likely to be less adiabatic ($\kappa \sim 10^{-3}$) than the ground-state exchange.[29] On the basis of these considerations the rate constant for electron exchange of the $^4T_2$ excited state with $Co(bpy)_3^+$ is estimated to be $10^{3\pm1}$ $M^{-1}$ $s^{-1}$. Similar considerations lead to the parameters for the $^2E$ excited state presented in Table V: in this case the nonadiabaticity of the electron exchange ($\kappa \sim 10^{-2}$) arises from the fact that the exchange involves transfer of an electron from $\sigma^*$d orbital, which

**Table V.** Properties of Low-Lying Excited States of $Co(bpy)_3^{2+}$

| state | electr config | band max,[a] eV ($\mu m^{-1}$) | $*E$,[b] eV | $k$,[c] $M^{-1}$ $s^{-1}$ | $\kappa$[d] |
|---|---|---|---|---|---|
| $^2T$ | $(\pi d)^5(\sigma^* d)^2$ [e] | 2.0 (1.6) | 2.0 | $1 \times 10^9$ | 1 |
| $^4T_2$ | $(\pi d)^4(\sigma^* d)^3$ | 1.4 (1.1) | 1.1 | $10^3$ | $10^{-3}$ |
| $^2E$ | $(\pi d)^6(\sigma^* d)^1$ | 0.55 (0.44) | 0.2 | $10^5$ | $10^{-2}$ |
| $^4T_1$[f] | $(\pi d)^5(\sigma^* d)^2$ | | | $1 \times 10^9$ | 1 |

[a] Transition energies for the $^2T$ and $^4T_2$ states from ref 31; the transition energy for the $^2E$ state was estimated by using the Tanabe–Sugano diagrams for $d^7$ systems and the *Dq* and *B* values for $Co(bpy)_3^{2+}$ presented in ref 31. [b] Energy of the thermally equilibrated excited state, calculated by substracting the distortion energy of the excited state from the (vertical) transition energy. [c] Rate constant for the cobalt(I)–cobalt(II) electron exchange. [d] Electronic transmission coefficient or degree of adiabaticity of the electron-exchange reaction. [e] The electronic configuration of the $^2T$ state was incorrectly assigned in ref 11. [f] Ground state of $Co(bpy)_3^{2+}$.

(28) (a) Values of $\lambda_{out}$ = 0.55 eV (calculated from the two-sphere model using $r$ = 13.6 Å) and $\lambda_{in}$ = 0.25 eV[28b] were used in calculating $\lambda$. See also the rate constants in Table V. (b) Szalda, D. J.; Creutz, C.; Mahajan, D.; Sutin, N. *Inorg. Chem.* **1983**, *22*, 2372. (c) Note that, in general, the electronic factors will also favor the formation of excited-state $RuL_3^{2+}$ since reactions in the inverted region are inherently nonadiabatic. See, e.g.: Sutin, N. *Acc. Chem. Res.* **1982**, *15*, 275.

(29) Sutin, N. *Prog. Inorg. Chem.* **1983**, *30*, 441.

(30) Indelli, M. T.; Ballardini, R.; Scandola, F. *J. Phys. Chem.* **1984**, *88*, 2547.

(31) Palmer, R. A.; Piper, T. S. *Inorg. Chem.* **1966**, *5*, 864.

(32) Szalda, D. J.; Macartney, D. H.; Sutin, N. *Inorg. Chem.* **1983**, *23*, 3473.

(33) (a) In order to estimate the energy of the thermally equilibrated excited states, a reduced mass of 32[32] and cobalt–nitrogen stretching frequencies of 230 and 300 $cm^{-1}$ were used for the $^4T_2$ and $^2E$ excited states, respectively. For comparison, the cobalt–nitrogen stretching frequencies of ground-state $Co(bpy)_3^{2+}$ and $Co(bpy)_3^{3+}$ are 266 and 378 $cm^{-1}$, respectively.[28] The frequencies used for the $^4T_2$ and $^2E$ excited states reflect the shifts expected for the change in the cobalt–nitrogen bond lengths (increases and decreases of 0.10–0.12 Å, respectively) on going from the ground to the excited states.[28] The reorganization energies were calculated from harmonic oscillator expressions. (b) The equilibrium constant for the high-spin/low-spin equilibrium in $Co(bpy)_3^{2+}$, calculated from the energy estimated for the thermally equilibrated $^2E$ excited state, is $10^{-3}$ to $10^{-4}$. This equilibrium constant is sufficiently large for a preequilibrium spin change on $Co(bpy)_3^{2+}$ to provide a competing mechanism for the $Co(bpy)_3^{2+}/Co(bpy)_3^{3+}$ electron exchange and is consistent with the spin equilibrium observed for $Co(terpy)_2^{2+}$.

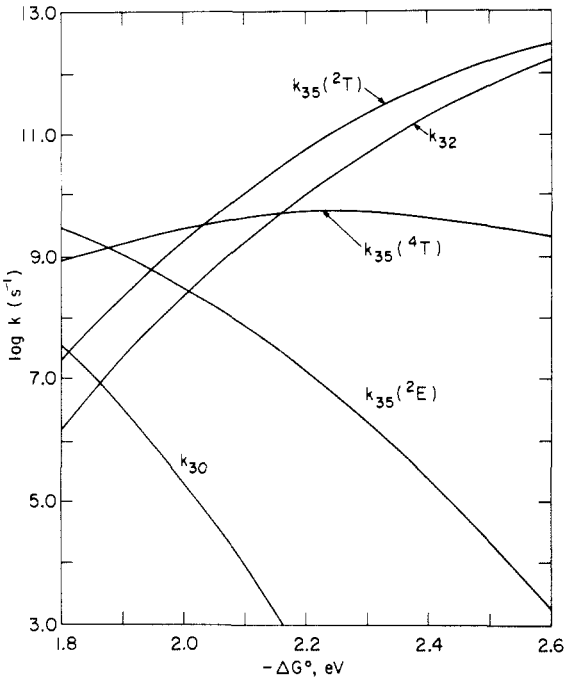


**Figure 2.** Plot of calculated first-order electron-transfer rate constants as a function of the (work uncorrected) driving force for the ground-state reaction (eq 2). The $k_{35}$ values refer to production of ground-state $RuL_3^{2+}$ and the excited ($^2T$, $^4T_2$, or $^2E$) $CoL_3^{2+}$, $k_{32}$ is for ground-state $CoL_3^{2+}$ and $^*RuL_3^{2+}$, and $k_{30}$ is for both $CoL_3^{2+}$ and $RuL_3^{2+}$ in the ground state. In addition to the values in Table V, the following exchange rates (0.1 M ionic strength, $CH_3CN$) and $\kappa$ values were used in the calculations: $RuL_3^{2+}/RuL_3^{3+}$, $3 \times 10^8$ $M^{-1}$ $s^{-1}$, 1; $^*RuL_3^{2+}/RuL_3^{3+}$, $3 \times 10^8$ $M^{-1}$ $s^{-1}$, 1; $CoL_3^{+}/CoL_3^{2+}$, $1 \times 10^9$ $M^{-1}$ $s^{-1}$, 1. These exchange rates were calculated from the values in 0.1 M aqueous medium by correcting for the effect of dielectric constant on the work and solvent reorganization terms, while the $\kappa$ values are the same as those employed previously.[11] The $\kappa$ values used for the cross-reactions are: $\kappa_{30} = 1$, $\kappa_{32} = 1$, $\kappa_{23} = 1$, $\kappa_{35}(^2E) = 10^{-2}$, $\kappa_{35}(^4T_2) = 10^{-3}$, $\kappa_{35}(^2T) = 1$. As in previous work,[11] the value of $k_{en}' = 1.2 \times 10^9$ $s^{-1}$, while the value of $k_{21}$, calculated from the diffusion equation, is $8.9 \times 10^9$ $s^{-1}$.

does not mix efficiently with the ligand $\pi^*$ orbitals.

The various pathways for the chemiluminescence reaction are summarized in Scheme I. This scheme illustrates the competing formation of the ground-state species, $RuL_3^{2+}|CoL_3^{2+}$ ($k_{30}$), and the excited-state species, $^*RuL_3^{2+}|CoL_3^{2+}$ ($k_{32}$) and $RuL_3^{2+}|^*CoL_3^{2+}$ ($k_{35}$). The rate constant $k_{35}$ is equal to the sum of $k_{35}(^2T)$, $k_{35}(^4T_2)$, and $k_{35}(^2E)$, and the formation of $^*CoL_3^{2+}$ is assumed to be irreversible because of the short lifetimes expected for these excited states.[34] Also included in Scheme I are the first-order pathways for oxidative ($k_{23}$), reductive ($k'_{red}$), and energy-transfer ($k'_{en}$) quenching of the $^*RuL_3^{2+}$ emission. The values of $k_{30}$, $k_{32}$, $k_{35}(^2T)$, $k_{35}(^4T_2)$, and $k_{35}(^2E)$ can be calculated from the modified cross-relation, eq 5,[11] where $k_{ii}$ and $k_{jj}$ are the rate constants for

$$k_{ij} = \kappa_{ij}(k_{ii}k_{jj}K_{ij}f_{ij}/\kappa_{ii}\kappa_{jj})^{1/2}W_{ij} \quad (5)$$

the exchange reactions, $k_{ij}$ and $K_{ij}$ are the rate and equilibrium constants for the cross-reaction, the $\kappa$'s are the nonadiabaticities of the reactions, $f_{ij}$ is a function of $k_{ii}$, $k_{jj}$, $\kappa_{ii}$, $\kappa_{jj}$, and $K_{ij}$, and $W_{ij}$ is a function of the work terms. Equation 5 yields second-order rate constants: the first-order rate constants were calculated by dividing the second-order rate constants by the equilibrium constant for the formation of $RuL_3^{3+}|CoL_3^{+}$ from $RuL_3^{3+}$ and $CoL_3^{+}$. The first-order rate constants obtained in this manner are plotted vs. the driving force for the reaction producing ground-state $RuL_3^{2+}$ and $CoL_3^{2+}$ in Figure 2. As expected, the rate constant calculated for the formation of ground-state products ($k_{30}$) is negligible compared with the rate constants calculated for the excited-state pathways ($k_{32}$ and $k_{35}$). It is also evident from Figure 2 that the reaction of $Ru(bpy)_3^{3+}$ with $Co(bpy)_3^{+}$ to yield the $^2E$ excited state of $Co(bpy)_3^{2+}$, which is the most exergonic of the reactions forming $^*Co(bpy)_3^{2+}$, lies in the inverted region. By contrast, the reaction forming the $^2T$ state is the least exergonic of the reactions forming $^*Co(bpy)_3^{2+}$ and lies in the normal region. Since this reaction is slightly more exergonic than that producing $^*RuL_3^{2+}$, the formation of $^*CoL_3^{2+}(^2T)$ competes successfully with $^*RuL_3^{2+}$ formation because, like the $^*Ru(bpy)_3^{2+}$ exchange, the $^2T$ exchange is very rapid. Interestingly, the reaction forming the $^4T_2$ state undergoes a transition from normal to inverted behavior in the free energy range considered.

A steady-state approximation for the concentrations of the various intermediates in Scheme I gives eq 6 for the yield of excited-state $^*RuL_3^{2+}$. In the application of eq 6 to the present

$$Y(^*Ru) = k_{21}k_{32}/[(k_{30} + k_{35}) \times (k_{21} + k_{23} + k'_{red} + k'_{en}) + k_{32}(k_{21} + k'_{red} + k'_{en})] \quad (6)$$

systems the $k'_{red}$ path is negligible[11] and $k_{12}$ can be calculated from the diffusion equation and the stability constant of the precursor complex.[35] The $^*RuL_3^{2+}$ yields calculated from eq 6 are 0.22, 0.17, and 0.08, respectively, for the first, second, and fourth reactions listed in Table IV. (The $Co(bpy)_3^{2+}$ parameters in Table V were used in all three yield calculations.) In view of the uncertainties in the experimental yields and the many assumptions of the model, the agreement is satisfactory. Moreover, the agreement can be further improved by small changes in the parameters. Thus the chemiluminescence yields are primarily determined by competition between $k_{32}$ and $k_{35}(^2T)$. The difference in the driving force for these two reactions is only 0.10 eV. Consequently, the relative rates of these reactions are very sensitive to the values used for the excited-state energies (cf. eq 3, note that the $\lambda$ and $\kappa$ values for the two reactions are the same). For example, increasing the excitation energy of the $^2T$ state from 2.00 to 2.03 eV changes the calculated chemiluminescence yields for the three reactions considered to 0.27, 0.23, and 0.11, respectively, thereby even further improving the agreement with the experimental yields.

Although the agreement with the experimental yields is gratifying and provides some justification for the model used, the various assumptions need to be kept in mind. First, evidence for the formation of excited cobalt(II) is indirect: althout it was also found necessary to invoke the formation of the $^2T$ state in an earlier study[11] of the quenching of $^*RuL_3^{2+}$ emission by $CoL_3^{2+}$ complexes and the properties assigned here to this excited state are reasonable, direct characterization of the excited cobalt(II) is desirable. Studies along these lines are under way. In addition, the calculated yields are sensitive to the driving forces and nonadiabaticities of the excited-state reactions and, for the reaction forming ground-state products, also to the work terms, which are difficult to determine: however, the parameters used are quite reasonable for reactions of this type.[28a,29] In any case, it is clear that appreciable yields of excited-state $RuL_3^{2+}$ are formed in the reaction of $RuL_3^{3+}$ with $CoL_3^{+}$ and that these yields require that reaction to form ground-state products be relatively slow.

The observed reaction patterns thus conform to the predictions of the classical Marcus formalism: the highly exergonic reaction to form ground-state products is slow, presumably because it lies in the inverted free energy region, and is unable to compete with the less exergonic, but noninverted, reactions that form excited-state products. The formation of electronically excited products in bimolecular reactions in turn provides good evidence for the existence of the inverted regime in such systems. While the existence of this regime has been convincingly demonstrated for intramolecular electron transfers,[36] evidence of inverted behavior

(34) The $^*CoL_3^{2+}$ excited states are assumed to be short lived: although the $^2T$ state is relatively undistorted and therefore not directly coupled to the ground state, it will be coupled to the ground state via the lower lying $^4T_2$ and $^2E$ states, which are considerably distorted (Stokes shifted). As a consequence the $^2T$ state, like the $^4T_2$ and $^2E$ states, is expected to have a short lifetime.

(35) Brunschwig, B. S.; Ehrenson, S.; Sutin, N. *J. Am. Chem. Soc.* **1984**, *106*, 6858.

(36) Miller, J. R.; Calcaterra, L. T.; Closs, G. L. *J. Am. Chem. Soc.* **1984**, *106*, 3047. Wasielewski, M. R.; Niemczyk, M. P.; Svec, W. A.; Pewitt, E. B. *J. Am. Chem. Soc.* **1985**, *107*, 1080.

in bimolecular electron transfers has been difficult to obtain.[37]

**Acknowledgment.** We thank M. Chou for assistance with some of the emission measurements. This work was performed at Brookhaven National Laboratory under contract DE-AC02-76CH00016 with the U.S. Department of Energy and supported by its Division of Chemical Sciences, Office of Basic Energy Sciences.

(37) Creutz, C.; Sutin, N. *J. Am. Chem. Soc.* **1977**, *99*, 241.

**Registry** No. $Ru(bpy)_3^{2+}$, 15158-62-0; $Ru(bpy)_3^{3+}$, 18955-01-6; $Ru(4,7\text{-}(CH_3)_2phen)_3^{2+}$, 24414-00-4; $Ru(4,7\text{-}(CH_3)_2phen)_3^{3+}$, 79747-03-8; $Os(terpy)_2^{2+}$, 85452-91-1; $Os(terpy)_2^{3+}$, 100815-62-1; $Co(bpy)_3^{+}$, 47780-35-8; $Co(4,4'\text{-}(CH_3)_2bpy)_3^{+}$, 47837-97-8; $Co(terpy)_2^{3+}$, 18308-16-2; $Co(terpy)_2^{+}$, 47779-83-9.

# Solvation Structure of a Sodium Chloride Ion Pair in Water

**Alan C. Belch,*† Max Berkowitz,*† and J. A. McCammon*‡**

*Contribution from the Departments of Chemistry, University of North Carolina, Chapel Hill, North Carolina 27514, and the University of Houston, Houston, Texas 77004.*
*Received June 13, 1985*

**Abstract:** Changes in the equilibrium solvation structure associated with the separation of a $Na^+Cl^-$ ion pair in water have been examined with use of computer simulation. At all separations, the $Na^+$ attempts to maintain an octahedral shell of nearest neighbors. This shell is comprised of five waters and the chloride in the stable contact ion pair. When the ions are separated slightly, the five waters rotate, weakening their hydrogen bonding with the second shell waters and producing a distorted octahedron. Those waters which rotate toward the chloride assume "bridging" orientations characterized by favorable electrostatic interactions with both ions. Further separation leads to replacement of the chloride by a sixth water molecule and formation of a stable solvent-separated ion pair in which strong hydrogen bonds are again formed between the first and second shells near $Na^+$. More subtle changes in structure and interactions occur farther from the $Na^+$ and around the $Cl^-$; these changes are noticeable up to about 7 Å from each ion.

## I. Introduction

The association of oppositely charged ions is an important step in many chemical reactions and in the formation and activity of many biological molecules.[1] Many rapid ionic reactions in solution apparently have very small barriers and therefore are diffusion controlled. The influence of strong electrostatic forces on the diffusive approach rate of ions was successfully studied by Onsager[2] and Debye[3] using continuum theories. Later, it became apparent that for ionic reactions with high barriers a more detailed level of microscopic description is necessary. Thus the idea of a solvent-separated ion pair $A^+||B^-$ separated by a barrier from the contact ion pair $A^+B^-$ was introduced by Fuoss[4] and Winstein.[5] The clarification of the role played by solvent in the process of ion pair interconversion from solvent-separated into close contact configurations is an important step in our understanding of chemical reactivity in solutions.

Because of the importance of water as a solvent, we concentrate on properties of ionic pairs in aqueous solutions. Recently we obtained the form of the potential of mean force for a sodium chloride ion pair in water using molecular dynamics computer simulation.[6] Distinct minima in the free energy of the system were found for contact and solvent separated ion geometries at 25 °C. In the present paper we report a detailed analysis of the solvation structure of the same system as a function of ion–ion distance. The method used in this work is outlined in section II. In section III, we discuss the results on structural and energetic changes in water around the ion pair. Section IV presents the concluding remarks.

## II. Method

Molecular dynamics simulations were carried out on a system of 295 TIPS2 water molecules and a single $Na^+Cl^-$ ion pair. The ions were held at fixed separation distances of 2.7, 3.7, 5.0, and 5.6 Å in successive simulations. These distances were selected from the minima and maxima of the potential of mean force calculated by Berkowitz et al.[6] The value

Table I. TIPS2 Parameters for Water, $Na^+$, and $Cl^-$

| site | $q$(electrons) | $10^{-3}A^2$, kcal Å$^{12}$/mol | $C^2$, kcal Å$^6$/mol |
|---|---|---|---|
| O in $H_2O$ | 0.000 | 695 | 600 |
| M in $H_2O$ | −1.070 | 0 | 0 |
| H in $H_2O$ | 0.535 | 0 | 0 |
| $Na^+$ | 1.0 | 14 | 300 |
| $Cl^-$ | −1.0 | 26 000 | 3500 |

2.7 Å represents the contact pair distance, 5.0 Å and 5.6 Å are solvent separated distances, and 3.7 Å is the distance at a maximum of the potential of mean force and therefore represents a transition-state region. The box for the simulation was rectangular; lengths of the sides were 18.6, 18.6, and 25.4 Å. The long dimension was chosen to be along the ion-pair separation vector so as to minimize artifacts associated with the use of periodic boundary conditions.

The potentials employed were the TIPS2 potential for the water–water interaction and similar TIPS2-like potentials for the ion–ion and ion–water interactions.[7] These potentials are of the form shown in eq 1. The

$$U_{mn} = \sum_{i \in m} \sum_{j \in n} \left( \frac{q_i q_j e^2}{r_{ij}} + \frac{A_i A_j}{r_{ij}^{12}} - \frac{C_i C_j}{r_{ij}^{6}} \right) \quad (1)$$

parameters for the potentials are shown in Table I. The interactions were truncated at 8.5 Å and polarization effects were not included. These potentials were shown to give a reliable representation of a solvation structure in single ion hydration.[7]

The dynamics were carried out with use of the Verlet algorithm with SHAKE[8] on a VAX 11/780. The time step was 4 fs and each configu-

† University of North Carolina.
‡ University of Houston.

(1) Lowry, T. H.; Richardson, K. S. "Mechanism and Theory in Organic Chemistry"; 2nd ed.; Harper and Row: New York, 1981.
(2) Onsager, L. *Phys. Rev.* **1938**, *54*, 554.
(3) Debye, P. *Trans. Electrochem. Soc.* **1942**, *82*, 265.
(4) Sadek, H.; Fuoss, R. *J. Am. Chem. Soc.* **1954**, *76*, 5897.
(5) Winstein, S.; Clippinger, E.; Fainberg, A. H.; Robinson, G. C. *J. Am. Chem. Soc.* **1954**, *76*, 2597.
(6) Berkowitz, M.; Karim, O. A.; McCammon, J. A.; Rossky, P. J. *Chem. Phys. Lett.* **1984**, *105*, 577.
(7) Jorgensen, W. L. *J. Chem. Phys.* **1982**, *77*, 4156. Jorgensen, W. L.; Madura, J. W.; Impey, R. W.; Klein, M. L. *J. Chem. Phys.* **1983**, *79*, 926. Jorgensen, W. L.; Chandrasekhar, J. *J. Chem. Phys.* **1982**, *77*, 5080.

0002-7863/86/1508-1755$01.50/0 